



Published in final edited form as:

*Surgery*. 2010 July ; 148(1): 87–95. doi:10.1016/j.surg.2009.12.004.

## Real-Time Intraoperative Near-Infrared Fluorescence Identification of the Extrahepatic Bile Ducts using Clinically-Available Contrast Agents

Aya Matsui, M.D.<sup>1,2</sup>, Eiichi Tanaka, M.D., Ph.D.<sup>1,2</sup>, Hak Soo Choi, Ph.D.<sup>1</sup>, Joshua H. Winer, M.D.<sup>3</sup>, Vida Kianzad, Ph.D.<sup>1</sup>, Sylvain Gioux, Ph.D.<sup>1</sup>, Rita G. Laurence, B.S.<sup>1</sup>, and John V. Frangioni, M.D., Ph.D.<sup>1,4,\*</sup>

<sup>1</sup>Division of Hematology/Oncology, Beth Israel Deaconess Medical Center, Boston, MA

<sup>2</sup>Division of Cancer Diagnostics and Therapeutics, Hokkaido University Graduate School of Medicine, Sapporo, Japan

<sup>3</sup>Department of Surgery, Brigham & Women's Hospital, Boston, MA

<sup>4</sup>Department of Radiology, Beth Israel Deaconess Medical Center, Boston, MA

### Abstract

**Background**—Iatrogenic bile duct injuries are serious complications with patient morbidity. We hypothesized that the invisible near-infrared (NIR) fluorescence properties of methylene blue (MB) and indocyanine green (ICG) could be exploited for real-time, intraoperative imaging of the extrahepatic bile ducts during open and laparoscopic surgeries.

**Methods**—2.0 mg/kg of MB and 0.05 mg/kg of ICG were intravenously injected into 35-kg female Yorkshire pigs and the extrahepatic bile ducts imaged over time using either the FLARE™ image-guided surgery system (open surgery) or a custom NIR fluorescence laparoscopy system. Surgical anatomy was confirmed using x-ray cholangiography. Contrast-to-background ratio (CBR), contrast-to-liver ratio (CLR), and chemical concentrations in the cystic duct (CD) and common bile duct (CBD) were measured, and the performance of each agent quantified.

© 2009 Mosby, Inc. All rights reserved.

\*To whom all correspondence should be addressed: John V. Frangioni, M.D., Ph.D., BIDMC, Room SL-B05, 330 Brookline Avenue, Boston, MA 02215, 617-667-0692 Fax: 617-667-0981, jfrangio@bidmc.harvard.edu.

**Publisher's Disclaimer:** This is a PDF file of an unedited manuscript that has been accepted for publication. As a service to our customers we are providing this early version of the manuscript. The manuscript will undergo copyediting, typesetting, and review of the resulting proof before it is published in its final citable form. Please note that during the production process errors may be discovered which could affect the content, and all legal disclaimers that apply to the journal pertain.

#### **Author Statements of Financial Interest:**

Aya Matsui, M.D.: None

Eiichi Tanaka, M.D., Ph.D.: None

Joshua H. Winer, M.D.: None

Vida Kianzad, Ph.D.: None

Sylvain Gioux, Ph.D.: None

Rita G. Laurence, B.S.: None

John V. Frangioni, M.D., Ph.D.: All intellectual property for the FLARE™ imaging system and the use of methylene blue for intraoperative NIR fluorescence imaging is owned by the Beth Israel Deaconess Medical Center (BIDMC), a teaching hospital of Harvard Medical School. As inventor of the technology, Dr. Frangioni may someday receive royalties if the technology is ever commercialized. Dr. Frangioni has no real or deferred equity interests, whatsoever, in this, or any other technology. Dr. Frangioni does not consult for any company. GE Healthcare sponsored research in Dr. Frangioni's laboratory, as specified above.

**Results**—Using NIR fluorescence of MB, the CD and CBD could be identified with good sensitivity (CBR and CLR  $\geq 4$ ), during both open and laparoscopic surgeries, from 10 to 120 min post-injection. Functional impairment of the ducts, including constriction and injury were immediately identifiable. Using NIR fluorescence of ICG, extrahepatic bile ducts did not become visible until 90 min post-injection due to strong residual liver retention, however, between 90 to 240 min, ICG provided exquisitely high sensitivity for both CD and CBD, with CBR  $\geq 8$  and CLR  $\geq 4$ .

**Conclusions**—We demonstrate that two clinically available NIR fluorophores, MB fluorescing at 700 nm and ICG fluorescing at 800 nm, provide sensitive, prolonged identification of the extrahepatic bile ducts and assessment of their functional status.

## INTRODUCTION

Cholecystectomy is one of the most frequently performed surgical procedures in the United States, with 398,000 laparoscopic cholecystectomies (LC) performed annually.<sup>1</sup> Although rare, iatrogenic bile duct injuries are serious complications with high patient morbidity. These injuries occur in approximately 0.18% to 0.5% of LC cases,<sup>2–4</sup> and 0.3% to 2.8% of open cholecystectomy (OC) cases.<sup>5–7</sup> To minimize the risk of injury, techniques such as the “critical view of safety,” described for by Strasberg and colleagues,<sup>8</sup> have been developed. However, adhesions or inflammation make clean surgical dissection difficult. To provide real-time intraoperative guidance, visible fluorescence-based methods have been described.<sup>9,10</sup> However, near-infrared (NIR) fluorescent light (700 to 900 nm), otherwise invisible to the human eye, offers several advantages over visible wavelength fluorescence for intraoperative bile duct imaging, including penetration of several millimeters into living tissue, high sensitivity detection, and low autofluorescence background.<sup>11</sup> Previously, we defined the parameters for an “optimal” NIR contrast agent.<sup>12</sup> Unfortunately, such optimal agents are 5 to 10 years away from clinical availability due to a variety of intellectual property, regulatory, and commercial issues beyond the control of academic investigators. In this study we hypothesized that two different NIR fluorophores, already FDA-approved for other indications, might provide adequate contrast for anatomical and functional assessment of the extrahepatic bile ducts after a simple intravenous injection.

## MATERIALS AND METHODS

### Reagents and Animals

Methylene blue (MB; methylene blue injection USP, 1%, 10 mg/ml, 31.3 mM) was purchased from Taylor Pharmaceuticals (Buffalo Grove, IL). Indocyanine green (ICG) was purchased from Akorn (Decatur, IL). Animals were studied under the supervision of an approved institutional protocol. Female Yorkshire pigs (E.M. Parsons and Sons, Hadley, MA) were 11 weeks old, with mean body weight 37.1 kg. Animals were induced with 4.4 mg/kg intramuscular Telazol™ (Fort Dodge Labs, Fort Dodge, IA), intubated, and maintained with 2% isoflurane (Baxter Healthcare Corp., Deerfield, IL). Electrocardiogram, heart rate, pulse oximetry (SpO<sub>2</sub>), and body temperature were monitored throughout surgery. A 14G central venous catheter was inserted into either the femoral vein or the external jugular vein, and saline was administered at 350 ml per hour.

### Measurement of Optical Properties

Absorbance and fluorescence of MB in bile were measured as described in detail previously,<sup>13</sup> except for absorbance measurements bile was diluted 20-fold in distilled water to lower background. For fluorescence quantum yield (QY) measurements of MB in bile, oxazine 725 in ethylene glycol (QY = 19%<sup>14</sup>) was used as a calibration standard under conditions of matched absorbance at 655 nm. For fluorescence QY measurements of ICG in bile, ICG in

dimethylsulfoxide (QY = 13% 15) was used as a calibration standard under conditions of matched absorbance at 770 nm.

### **NIR Fluorescence Imaging System for Open Surgery**

The Fluorescence-Assisted Resection and Exploration (FLARE™) image-guided surgery system has been described in detail previously,<sup>16</sup> as has its high-powered light emitting diode (LED) light source and filtration.<sup>17</sup> White light (400 to 650 nm), 670 nm excitation, and 760 nm excitation fluence rates used for this study were 0.6, 2.5, and 10.0 mW/cm<sup>2</sup>, respectively. Color video and two independent channels (700 nm and 800 nm) of NIR fluorescence images were acquired simultaneously at rates up to 15 Hz over a 15-cm diameter field-of-view using custom software.<sup>16</sup>

### **NIR Fluorescence Imaging System for Laparoscopic Surgery**

Light from a custom 300W Xenon light source (Wilson Associates, Weymouth, MA), equipped with filtration to remove all NIR and infrared light, was combined with light from a 500 mW 670 nm laser diode (Thor Labs, Newton, NJ) through a custom light mixer (Qioptiq Imaging Solutions, Rochester, NY), then through a 0.6 NA fiber optic cable to illuminate a standard rigid laparoscope (10 mm diameter, 0°; Storz, Tuttlingen, Germany). The eyepiece of the laparoscope was attached to custom optics (Qioptiq Imaging Solutions, Fairport, NY), which permitted simultaneous acquisition of color video and NIR light using a HV-D27 (Hitachi, Woodbury, NY) color CCD camera and Orca-AG (Hamamatsu, Bridgewater, NJ) NIR camera. A schematic and photo of the laparoscopic device is presented in Matsui et al. (companion article, in review).

### **Intraoperative Extrahepatic Bile Duct Imaging and Quantitative Assessment**

For open surgery experiments, a standard midline laparotomy was performed and a right transrectus incision was added. A 16 gauge central venous catheter was inserted into the stomach and was guided into the duodenum through the incised posterior wall of the duodenum at approximately 1 cm distal to the pylorus. The catheter, placed retrograde into the CBD via the papilla of Vater and fixed to the duodenal mucosa with 5-0 vicryl, was used to sample bile. The incised duodenal wall was closed with 5-0 vicryl.

A total of 8 animals were used. 4 animals were administered 2.0 mg/kg MB diluted in 30 ml saline as a 5 min infusion, and the other 4 were administered 0.05 mg/kg of ICG as a bolus diluted in total 10 ml saline. The imaging system was positioned 18" above the surgical field. In the MB group, images were recorded at the time of injection (T = 0 min), then every 5 min for 10 to 120 min post-injection using a camera exposure time of 150 to 250 msec. In the ICG group, images were recorded at the time of injection (T = 0 min), then 5, 10, 30, 60, 70 min post-injection, then every 10 min for 90 to 240 min post-injection using a camera exposure time of 30 to 60 msec. All images were taken at end expiration to minimize movement artifact.

At each time point, the fluorescence intensity (FI) and background (BG) intensity of a region of interest (ROI) over the CBD and CD were quantified using custom software. The performance metrics for MB fluorescence were the contrast-to-background ratio (CBR) and contrast-to-liver ratio (CLR); where exposed rectus muscle was used as background.  $CBR = (FI \text{ of ROI} - BG \text{ intensity})/BG \text{ intensity}$ .  $CLR = (FI \text{ of ROI} - FI \text{ of liver})/FI \text{ of liver}$ .

In the MB group, bile was collected prior to injection and every 15 min from 15 to 120 min post-injection. In the ICG group, bile was collected prior to injection, 10 min post-injection, and every 30 min from 30 to 240 min post-injection. Optical properties of collected bile were immediately measured after the experiments. For quantification of MB and ICG concentrations in bile, calibration solutions of each were prepared in swine bile, and samples quantified using

a VersaMax microplate reader (Molecular Devices, Sunnyvale, CA). Absorbance was measured at 668 nm for MB and 780 nm for ICG. Correlations between the concentration of MB or ICG in bile, and the CBR of the liver, were evaluated statistically.

### **NIR Fluorescence-Guided Laparoscopic Imaging of the Extrahepatic Bile Ducts**

For laparoscopic surgery experiments, 4 animals were used. A small right subcostal incision was made and a 10 Fr catheter was inserted directly into the gallbladder fundus. The catheter was sutured to the gallbladder wall and left as percutaneous transhepatic gallbladder drainage (PTGBD) and for direct infusion of NIR fluorescent and iodine-based contrast agents. After the subcostal incision was closed, 4 ports were inserted according to the standard of care in LC. The abdominal cavity was insufflated with carbon dioxide, and the custom NIR laparoscope was inserted into the umbilical port. The fundus of the gallbladder was retracted cephalad to stretch the CD, then animals were injected with 2 mg/kg MB diluted in 30 ml of saline as a 5 min infusion. Images were recorded at the time of the injection (T = 0 min), and 10, 20, and 30 min post-injection using a camera exposure time of 500 msec. Subsequently, animals had 5 ml of 10  $\mu$ M MB solution in saline infused into the gallbladder via the PTGBD tube and a 5 mm clip was intentionally placed on the CBD identified using NIR fluorescence. After images were recorded with the clip, an injury was created on the CBD that penetrated into the CBD lumen, and 5 ml of 10  $\mu$ M MB solution was again infused into PTGBD tube. X-ray cholangiography was performed to confirm anatomical orientation using C-arm fluoroscopy (Series 9400 X-ray Imaging System, GE Healthcare, Princeton, NJ) using 5 ml of an iodine contrast agent (Renografin®-60, Bracco Diagnostics, Princeton, NJ) infused into the PTGBD tube.

### **Statistical Analysis**

Results were presented as mean  $\pm$  SEM. Correlation was studied using the two-tailed Pearson test with a 95% confidence interval.

## **RESULTS**

### **Optical Properties of MB and ICG**

The chemical structures of MB and ICG, and their key optical properties measured in swine bile, are shown in Figure 1A. MB is a compact, “700 nm” NIR fluorophore with only a modest extinction coefficient and a quenching threshold of 20  $\mu$ M. ICG, on the other hand, is a rather large, “800 nm” heptamethine indocyanine, with a 2-fold higher extinction coefficient and a quenching threshold of 10  $\mu$ M. Its superior excitation and emission wavelengths result in higher photon transmission and lower autofluorescence background in living tissue (see below).

### **Intraoperative NIR Fluorescence Imaging Systems**

Optical light paths and filtration for the FLARE™ open surgery imaging system are shown in Figure 1B. Key features of the system are the ability to acquire color video (i.e., 400 to 650 nm “white” light) images simultaneously with NIR fluorescence images, high frame rates (up to 15 Hz), a large field-of-view (FOV) of 15 cm, a long working distance (18”), and the use of safe LED light. Fluence rates used for this study were 0.6 mW/cm<sup>2</sup> for white light and 2.5 mW/cm<sup>2</sup> for 670 nm excitation light. The laparoscopic imaging system had similar design and performance, although laser light was required for fluorescence excitation due to the relatively low NIR transmission of the fiber optics.

### **Real-Time NIR Fluorescence Imaging of the Extrahepatic Bile Ducts during Open Surgery**

The FLARE™ intraoperative NIR fluorescence imaging system was configured as detailed in Figure 1B. This configuration permitted simultaneous acquisition of color video and two

independent channels of NIR fluorescence (centered at 700 nm and 800 nm), although only one NIR channel was used for individual experiments.

After a single intravenous injection, via either a peripheral or central venous line, the extrahepatic bile ducts were successfully imaged in all animals using both MB (Figure 2A) and ICG (Figure 2B). However, important differences between the two contrast agents were found. Optically, ICG provided a higher signal-to-background ratio (SBR) due to its higher extinction coefficient and QY, higher fluence rate available on FLARE™, and lower tissue autofluorescence. However, MB had much lower uptake in liver, and therefore a higher CLR in the CD and CBD at early time points. The most profound differences between the two agents, however, were their kinetics. MB signal intensity in the CD (Figure 3A) and CBD (Figure 3B) became visible within minutes and remained adequate for imaging for up to 120 min. ICG, on the other hand, required a long lag time ( $\geq 90$  min) before adequate contrast in the CD and CBD could be seen relative to liver, with the signal lasting for up to 240 min post-injection. Although the CBR and CLR for MB and ICG were roughly equivalent at later time points after injection (Figures 3A and 3B), the use of ICG's 800 nm fluorescence has the advantage of lower autofluorescence from surrounding bowel and tissue (e.g., compare Figure 2A to Figure 2B).

The NIR fluorescence signal intensity seen in liver did not correlate statistically ( $r = 0.2951$ ,  $p = 0.0806$ ) with MB concentration in bile, but did correlate ( $r = 0.5339$ ,  $p = 0.0011$ ) with ICG concentration in the bile (Figure 3C; discussed below).

### Real-Time NIR Fluorescence Imaging of the Extrahepatic Bile Ducts during Laparoscopic Surgery

The custom NIR fluorescence laparoscopy system was tested with MB, since it represents a “worst case” scenario for signal intensity. After a single intravenous injection of 2 mg/kg MB, the CD and CBD were identifiable from 10 min to 120 min post-injection in all animals, although a longer exposure time was required to compensate for losses in the optics. A representative image is shown in Figure 4A (top row). After purposeful mis-application of a surgical clip and infusion of 10  $\mu$ M MB into the PTGBD catheter, NIR fluorescence permitted ready identification of interrupted bile flow (Figure 4A, middle row). After purposeful injury to the CBD, NIR fluorescence also provided immediate identification of the problem and pinpointed the location of the leak (Figure 4A, bottom row). X-ray cholangiography using iodine contrast injected into the PTGBD confirmed that the surgical anatomy suggested by NIR fluorescence imaging was correct (Figure 4B).

## DISCUSSION

This study exploits invisible NIR fluorescent light, and the natural clearance mechanisms of MB and ICG, to provide surgeons with real-time, intraoperative identification of the extrahepatic bile ducts. After a single intravenous injection, MB is cleared simultaneously by liver and kidneys, resulting in high NIR fluorescence of the bile and urine, respectively. ICG, on the other hand, is cleared rapidly and efficiently by the liver, with an extremely brief ( $\leq 3.4$  min<sup>18</sup>) half-life in blood. The high liver uptake requires almost 2 hr before the fluorescence of ICG in bile exceeds that of liver, and resulted in a statistical correlation between NIR fluorescence in liver and subsequent ICG excretion into bile (Figures 3B and 3C).

Although both contrast agents provide sensitive and prolonged imaging, each has pros and cons. MB has the advantage of rapid excretion into bile and low signal intensity in the liver, but optical properties are modest and 700 nm emission is subject to higher autofluorescence background. ICG has the advantages of superior optical properties and lower dosing, but requires over 2 hr before imaging is optimal. In general, ICG is a better choice for bile duct



imaging if there is adequate time for clearance (i.e., at least 2 hr), and residual NIR fluorescence in the liver will not interfere with the desired dissection. MB is a better choice when bile duct contrast needs to be generated immediately, or when the surgical procedure involves the liver.

It should be noted that our use of MB as an invisible NIR fluorophore requires only micromolar final concentrations, and is distinctly different from MB's typical use as a visible blue dye, 19–21 which requires millimolar concentrations. In fact, increasing the intravenously injected dose of MB or ICG beyond what was reported here results in fluorescence quenching, due to dye stacking and/or internal absorption, and a paradoxical loss of fluorescence intensity. Keeping administered doses low also minimizes the risk of adverse reactions. Adverse reactions to both MB and ICG are more common at higher doses, although rapid infusion of up to 5 mg/kg of MB is tolerated by dogs,<sup>22</sup> and adverse reactions to ICG occur mainly at doses  $\geq 0.5$  mg/kg and in the setting of end stage renal disease.<sup>23</sup> The optimal doses required by our study (2 mg/kg for MB and 0.05 mg/kg for ICG) appear to fall below these thresholds. Dose can be lowered even further by increasing NIR fluorescence excitation fluence rate, although care must be taken with MB excitation to avoid tingeing the field with a reddish hue. MB should be avoided in subjects with known glucose-6-dehydrogenase deficiency (G6PD) due to the risk of severe hemolysis.<sup>24</sup>

Neither MB nor ICG are optimal contrast agents, though, for bile duct imaging. In a previous report, we demonstrated that the carboxylic acid of IRDye™800-CW was a near optimal agent exhibiting 800 nm fluorescence, high extinction coefficient, high quantum yield, rapid onset of NIR fluorescence signal, and prolonged imaging.<sup>12</sup> However, agents such as this that are not yet FDA-approved will be subject to long, costly, and complex regulatory hurdles. On the contrary, MB and ICG have been FDA-approved for other indications for over 50 years each, and are available clinically for further study.

Although an encouraging proof-of-principle, our results with NIR fluorescence laparoscopy are far from optimal. Commercially available laparoscopes generally have poor transmission of NIR wavelengths, and have not been engineered with wavelength correction to maintain focus between color and NIR channels. The present version of our custom optics is bulky, and does not provide image intensification to compensate for relatively low camera quantum efficiency in the NIR. Although some of these deficiencies could be compensated for by a longer camera exposure time, future studies must employ improved imaging system designs.

Another consideration when interpreting our study is the anatomical differences between pig and human. The hepatoduodenal ligament of a healthy pig is thinner than human, and it is presently unknown how well the extrahepatic bile ducts will be visualized in the setting of severe inflammation and adhesions. Fortunately, NIR light is capable of penetrating several millimeters into normal and inflamed tissue, and with proper choice of contrast agent, fluence rate, and camera exposure time, it should be possible to follow antegrade flow of bile from liver to the duodenum under many clinical scenarios. At the very least, NIR fluorescence imaging using the FLARE™ imaging system and MB and/or ICG should help lower the learning curve and complication rate for surgeons in training by providing real-time visualization of bile duct lumens in the context of surgical anatomy.

## Acknowledgments

We thank Barbara L. Clough for editing and Lorissa A. Moffitt and Eugenia Trabucchi for administrative assistance. This study was funded in part by National Institutes of Health (National Cancer Institute) grant #R01-CA-115296 and a sponsored research agreement from GE Healthcare.

## Abbreviations

BG	background
CBD	common bile duct
CBR	contrast-to-background ratio
CD	cystic duct
CLR	contrast-to-liver ratio
ECG	electrocardiogram
FI	fluorescence intensity
FOV	field-of-view
ICG	indocyanine green
IOC	intraoperative cholangiography
LC	laparoscopic cholecystectomy
LED	light emitting diode
MB	methylene blue
NIR	near-infrared
OC	open cholecystectomy
PTGBD	percutaneous transhepatic gallbladder drainage
QY	quantum yield
ROI	region of interest
SBR	signal-to-background ratio

## REFERENCES

1. Advance Data No. 385, Table 8. Number of all-listed procedures for discharges from short-stay hospitals by procedure category and age: United States, 2005. U.S. Department of Health and Human Services, Centers for Disease Control and Prevention, National Center for Health Statistics; 2007.
2. Flum DR, Dellinger EP, Cheadle A, Chan L, Koepsell T. Intraoperative cholangiography and risk of common bile duct injury during cholecystectomy. *Jama* 2003;289:1639–1644. [PubMed: 12672731]
3. Nuzzo G, Giuliani F, Giovannini I, Ardito F, D'Acapito F, Vellone M, et al. Bile duct injury during laparoscopic cholecystectomy: results of an Italian national survey on 56 591 cholecystectomies. *Arch Surg* 2005;140:986–992. [PubMed: 16230550]
4. Savassi-Rocha PR, Almeida SR, Sanches MD, Andrade MA, Ferreira JT, Diniz MT, et al. Iatrogenic bile duct injuries. *Surg Endosc* 2003;17:1356–1361. [PubMed: 12811663]
5. Buanes T, Mjaland O, Waage A, Langeeggen H, Holmboe J. A population-based survey of biliary surgery in Norway. Relationship between patient volume and quality of surgical treatment. *Surg Endosc* 1998;12:852–855. [PubMed: 9602005]
6. Diamantis T, Tsigris C, Kiriakopoulos A, Papalambros E, Bramis J, Michail P, et al. Bile duct injuries associated with laparoscopic and open cholecystectomy: an 11-year experience in one institute. *Surg Today* 2005;35:841–845. [PubMed: 16175465]
7. Van de Sande S, Bossens M, Parmentier Y, Gigot JF. National survey on cholecystectomy related bile duct injury--public health and financial aspects in Belgian hospitals--1997. *Acta Chir Belg* 2003;103:168–180. [PubMed: 12768860]
8. Strasberg SM, Eagon CJ, Drebin JA. The "hidden cystic duct" syndrome and the infundibular technique of laparoscopic cholecystectomy--the danger of the false infundibulum. *J Am Coll Surg* 2000;191:661–667. [PubMed: 11129816]

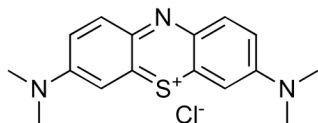
9. Holzinger F, Krahenbuhl L, Schteingart CD, Ton-Nu HT, Hofmann AF. Use of a fluorescent bile acid to enhance visualization of the biliary tract and bile leaks during laparoscopic surgery in rabbits. *Surg Endosc* 2001;15:209–212. [PubMed: 11285970]
10. Holzinger F, Schteingart CD, Ton-Nu HT, Eming SA, Monte MJ, Hagey LR, et al. Fluorescent bile acid derivatives: relationship between chemical structure and hepatic and intestinal transport in the rat. *Hepatology* 1997;26:1263–1271. [PubMed: 9362371]
11. Frangioni JV. In vivo near-infrared fluorescence imaging. *Curr Opin Chem Biol* 2003;7:626–634. [PubMed: 14580568]
12. Tanaka E, Choi HS, Humblet V, Ohnishi S, Laurence RG, Frangioni JV. Real-time intraoperative assessment of the extrahepatic bile ducts in rats and pigs using invisible near-infrared fluorescent light. *Surgery* 2008;144:39–48. [PubMed: 18571583]
13. Frangioni JV, Kim SW, Ohnishi S, Kim S, Bawendi MG. Sentinel lymph node mapping with type-II quantum dots. *Methods Mol Biol* 2007;374:147–159. [PubMed: 17237537]
14. Sens R, Drexhage KH. Fluorescence quantum yield of oxazine and carbazine laser dyes. *J Luminesc* 1981;24:709–712.
15. Benson C, Kues HA. Absorption and fluorescence properties of cyanine dyes. *J Chem Eng Data* 1977;22:379–383.
16. Troyan SL, Kianzad V, Gibbs-Strauss SL, Gioux S, Matsui A, Oketokoun R, et al. The FLARE™ intraoperative near-infrared fluorescence imaging system: a first-in-human clinical trial in breast cancer sentinel lymph node mapping. *Ann Surg Oncol* 2009;16:2943–2952. [PubMed: 19582506]
17. Gioux S, Kianzad V, Ciocan R, Gupta S, Oketokoun R, Frangioni JV. High-power, computer-controlled, light-emitting diode-based light sources for fluorescence imaging and image-guided surgery. *Mol Imaging* 2009;8:156–165. [PubMed: 19723473]
18. Cherrick GR, Stein SW, Leevy CM, Davidson CS. Indocyanine green: observations on its physical properties, plasma decay, and hepatic extraction. *J Clin Invest* 1960;39:592–600. [PubMed: 13809697]
19. Simmons R, Thevarajah S, Brennan MB, Christos P, Osborne M. Methylene blue dye as an alternative to isosulfan blue dye for sentinel lymph node localization. *Ann Surg Oncol* 2003;10:242–247. [PubMed: 12679308]
20. Han N, Bumpous JM, Goldstein RE, Fleming MM, Flynn MB. Intra-operative parathyroid identification using methylene blue in parathyroid surgery. *Am Surg* 2007;73:820–823. [PubMed: 17879694]
21. Marion JF, Waye JD, Present DH, Israel Y, Bodian C, Harpaz N, et al. Chromoendoscopytargeted biopsies are superior to standard colonoscopic surveillance for detecting dysplasia in inflammatory bowel disease patients: a prospective endoscopic trial. *Am J Gastroenterol* 2008;103:2342–2349. [PubMed: 18844620]
22. Traynor S, Adams JR, Andersen P, Everts E, Cohen J. Appropriate timing and velocity of infusion for the selective staining of parathyroid glands by intravenous methylene blue. *Am J Surg* 1998;176:15–17. [PubMed: 9683125]
23. Benya R, Quintana J, Brundage B. Adverse reactions to indocyanine green: a case report and a review of the literature. *Cathet Cardiovasc Diagn* 1989;17:231–233. [PubMed: 2670244]
24. Clifton J 2nd, Leikin JB. Methylene blue. *Am J Ther* 2003;10:289–291. [PubMed: 12845393]



A.

700 nm NIR Fluorophore

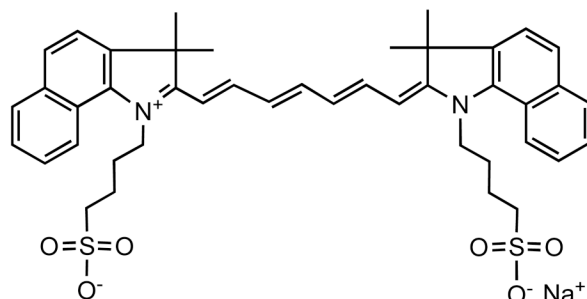
## Methylene Blue (MB)



M.W. 320 Da  
 Excitation Peak: 668 nm  
 Extinction Coefficient ( $M^{-1}cm^{-1}$ ): 53,300  
 Emission Peak: 688 nm  
 Quenching Threshold: 20  $\mu M$   
 Quantum Yield: 4.7%

800 nm NIR Fluorophore

## Indocyanine Green (ICG)



M.W. 776 Da  
 Excitation Peak: 806 nm  
 Extinction Coefficient ( $M^{-1}cm^{-1}$ ): 109,000  
 Emission Peak: 832 nm  
 Quenching Threshold: 10  $\mu M$   
 Quantum Yield: 4.0%

B.

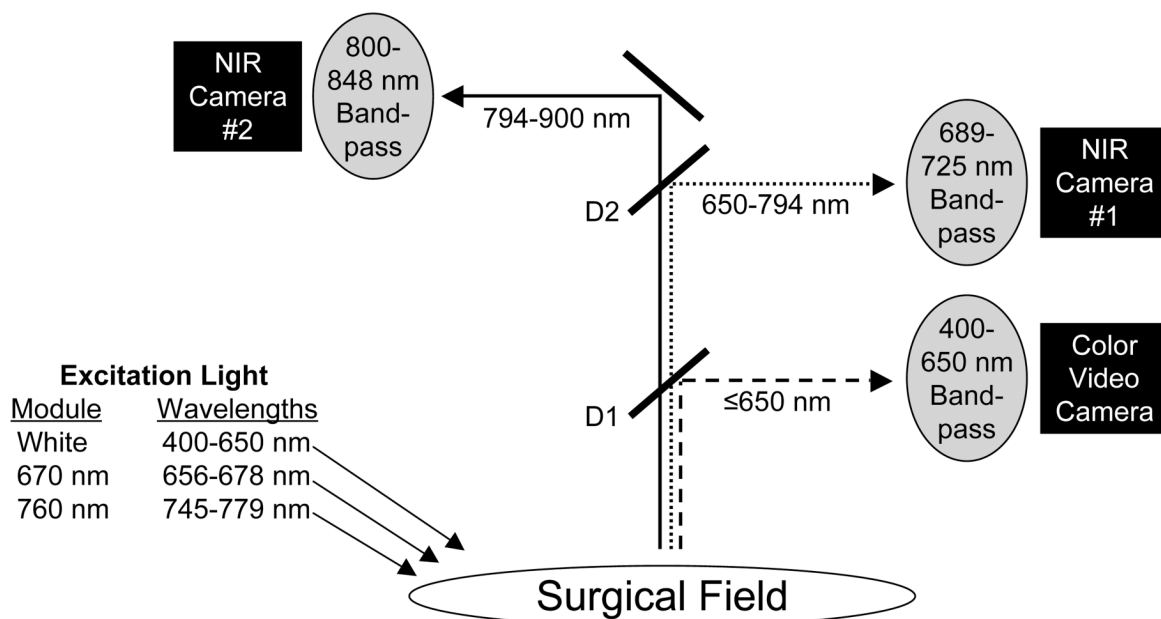


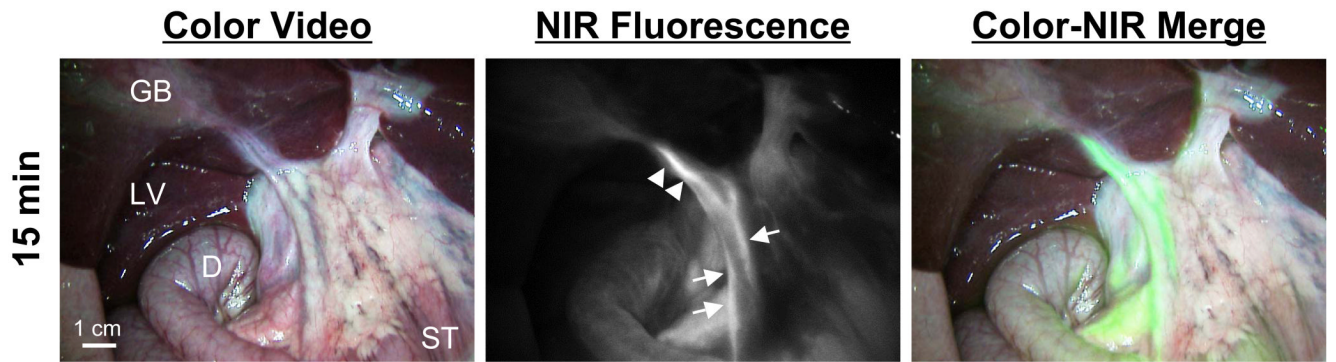
**Figure 1. NIR Fluorescent Contrast Agents and Imaging System Configuration**

A. Chemical structures and optical properties of methylene blue (MB) and indocyanine green (ICG) in swine bile.

B. The optical paths, dichroic mirrors (D1, D2), and filtration for the FLARE™ image-guided open surgery system used in this study. Filter wavelength ranges (nm) are provided for all excitation and emission filters. D1 = 680 nm center-wavelength dichroic mirror. D2 = 770 nm center-wavelength dichroic mirror.

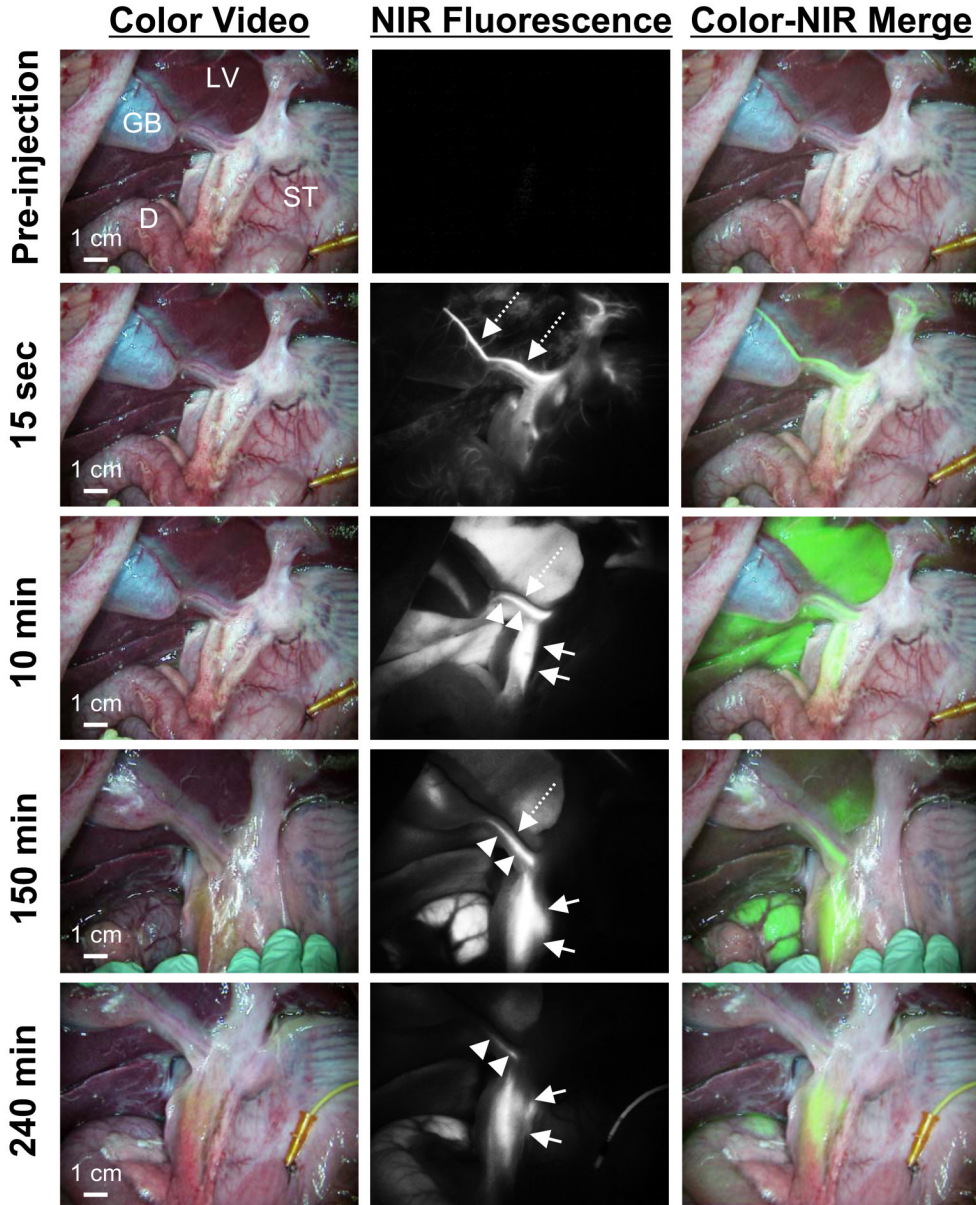
A.

**700 nm NIR Fluorophore (MB)**



**B.**

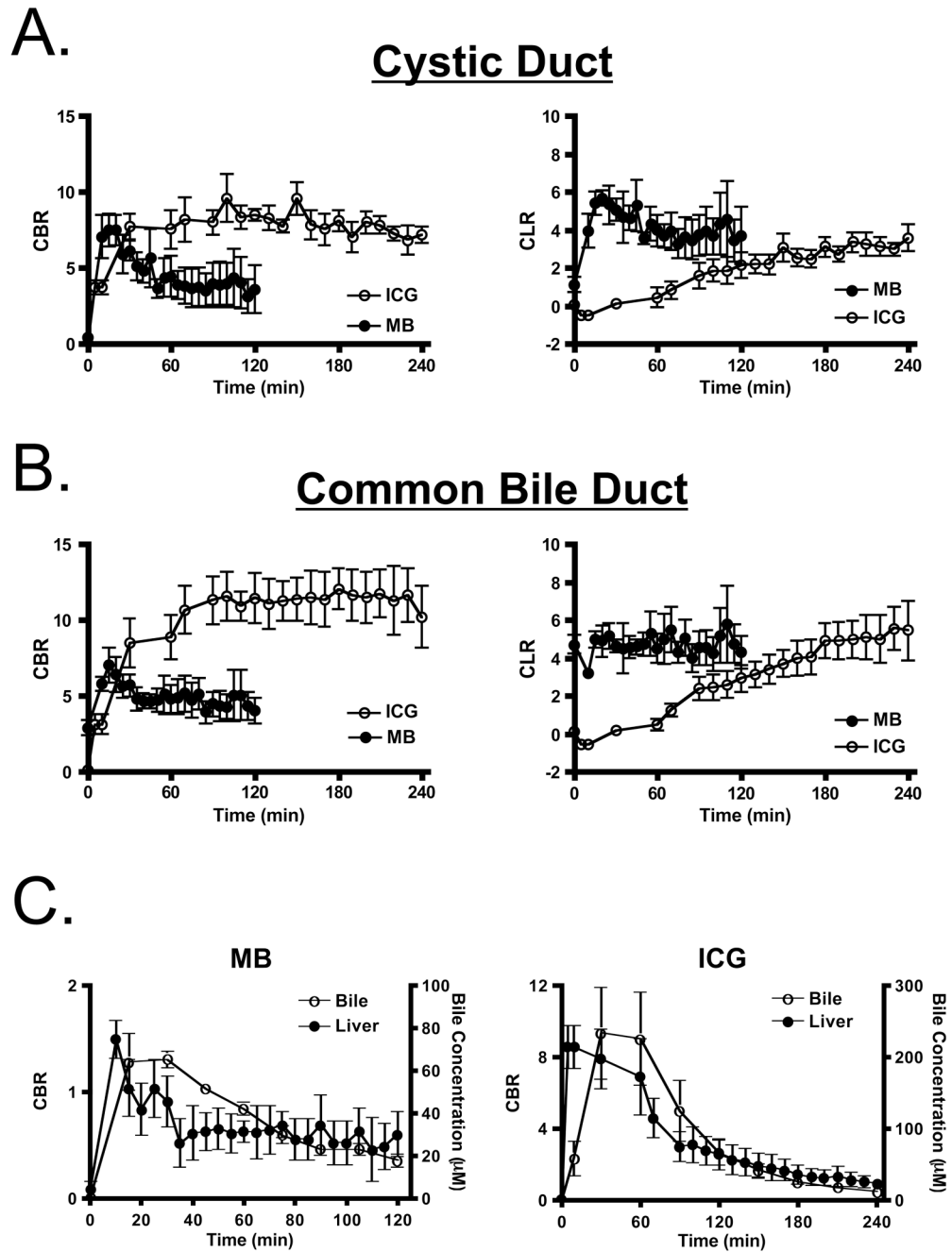
**800 nm NIR Fluorophore (ICG)**



**Figure 2. NIR Fluorescence-Guided Intraoperative Identification of the Extrahepatic Bile Duct** Shown are the color video (left column), NIR fluorescence (middle column), and a pseudo-colored (lime green) merged image of the two (right column). Arrows, dashed arrows, and arrowheads indicate the common bile duct, cystic artery, and cystic duct, respectively. The cystic artery appears black at time points later than 15 sec post-injection. GB: gallbladder, LV: liver, ST: stomach, D: duodenum.

A. 700 nm NIR fluorescence of 2.0 mg/kg MB at 15 min post-injection. Exposure time was 150 msec for the NIR fluorescence image.

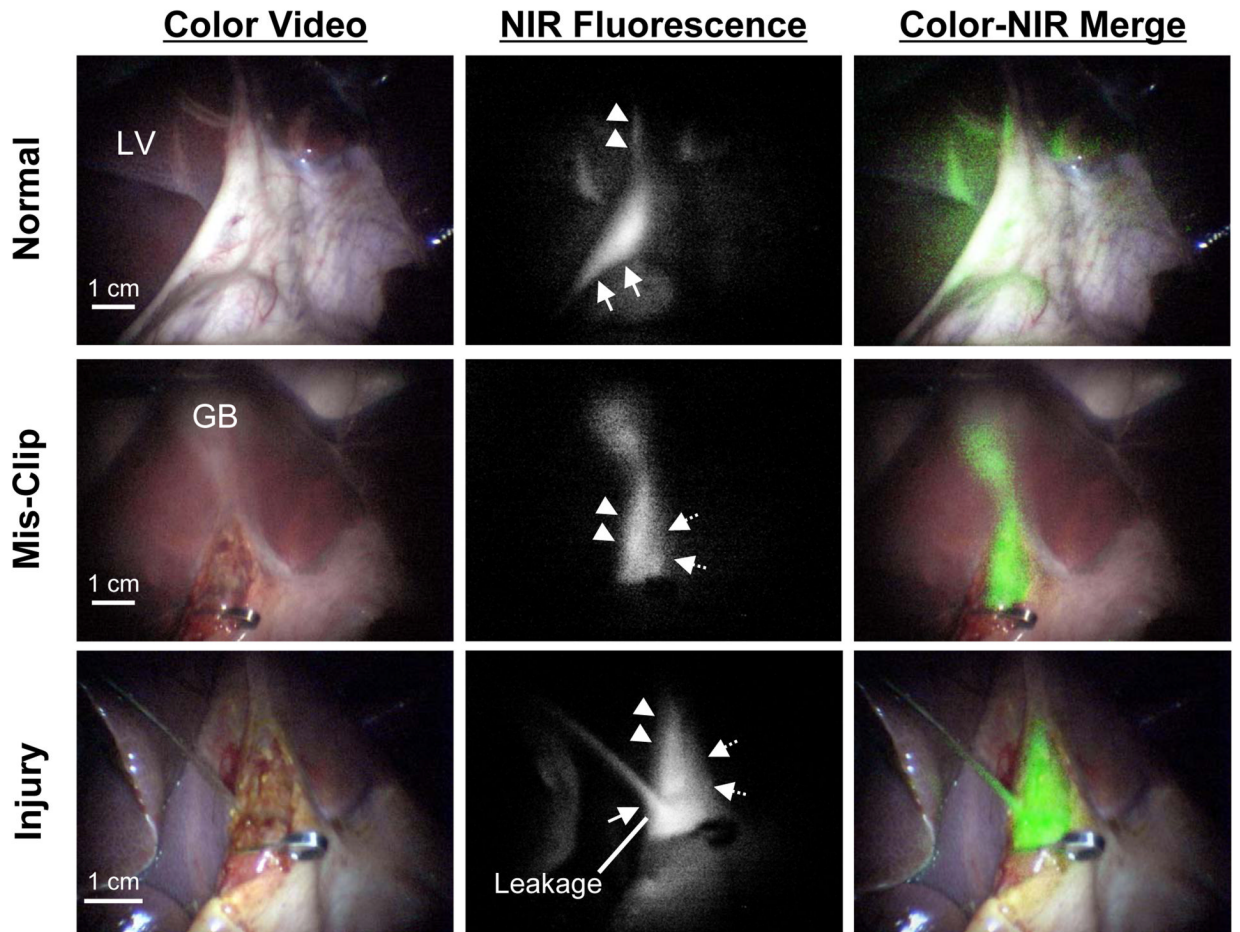
B. 800 nm NIR fluorophore 0.05 mg/kg ICG at the post-injection times indicated. Exposure time was 30 msec for all NIR fluorescence images.



**Figure 3. Quantitative Assessment of Extrahepatic Bile Duct Imaging using NIR Fluorescence**  
 A. Direct comparison of CBR (mean ± SEM; left) and CLR (mean ± SEM; right) between MB (closed circles) and ICG (open circles) in the cystic duct. CBR and CLR were obtained from images taken with an exposure time of 150 msec for MB and 30 msec for ICG.  
 B. Direct comparison of CBR (mean ± SEM; left) and CLR (mean ± SEM; right) between MB (closed circles) and ICG (open circles) in the common bile duct, as described in Figure 3A.  
 C. Correlation between imaging CBR (mean ± SEM) and actual NIR fluorophore concentration (mean ± SEM) in the liver (closed circles) and bile (open circles) for MB (left) and ICG (right). All image pixel intensities were within the linear range of the cameras.



A.





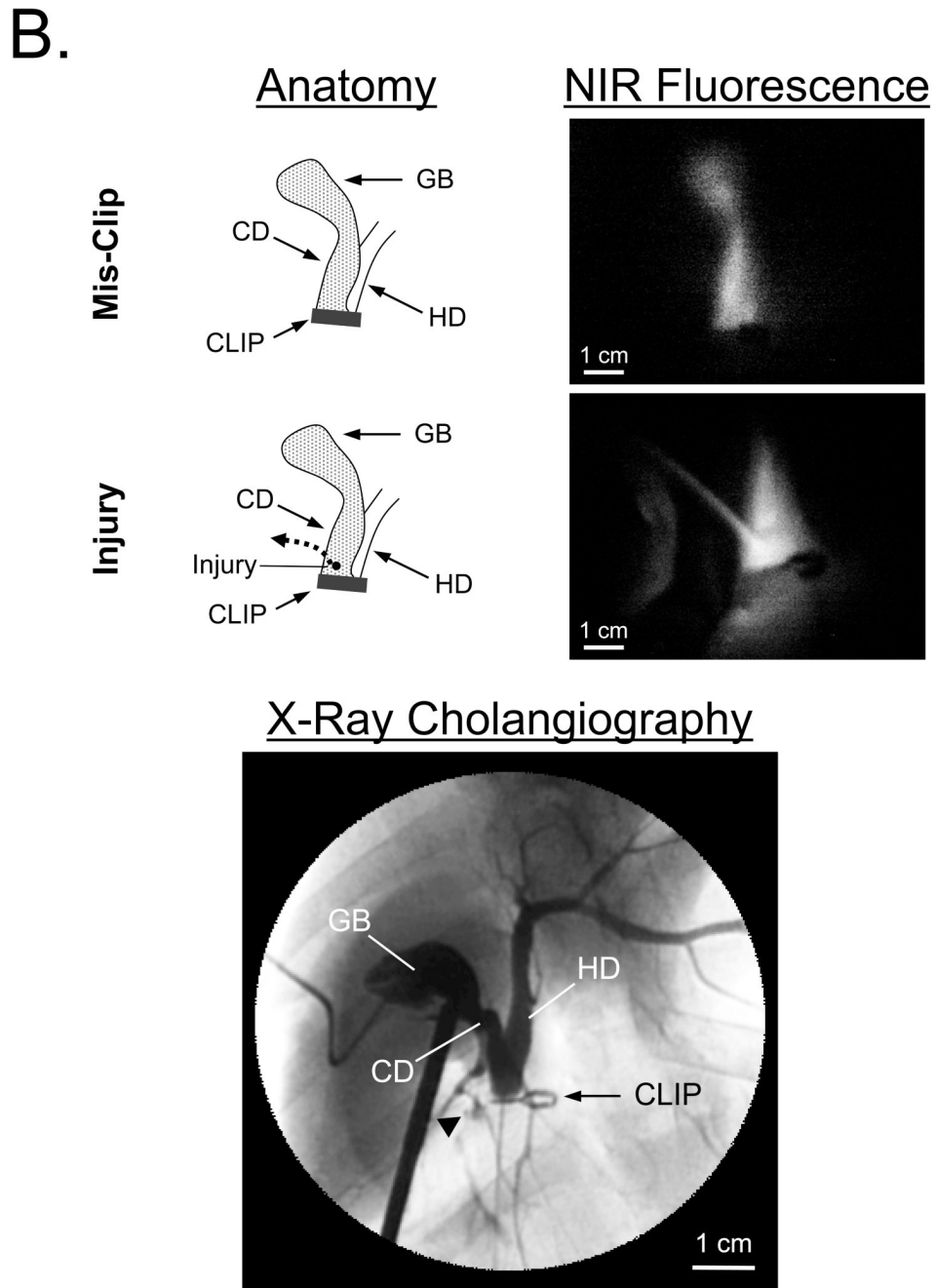


**Figure 4. Intraoperative NIR Fluorescence-Guided Extrahepatic Bile Duct Imaging during Laparoscopy**

A. Laparoscopic NIR fluorescence-guided extrahepatic bile duct imaging. Images include color video (left column), NIR fluorescence (middle column), and a pseudo-colored (lime green) merged image of the two (right column). Top row images are from 10 min post-injection of 2 mg/kg MB, with the gallbladder retracted upward, and out of, the field of view. Middle row images present the common bile duct mis-clipped at slightly below the origin of the cystic duct. Bottom row images show an injury to the common bile duct and leakage of MB solution from the injured hole. All NIR fluorescence images were taken with an exposure time 500

msec. Arrow, dashed arrow, and arrowhead indicate the common bile duct, common hepatic duct, and cystic duct, respectively. LV: liver, GB: gallbladder.

B. Verification of the surgical anatomy seen using NIR fluorescence laparoscopy by x-ray cholangiography. Schematic and NIR fluorescence images after mis-application of a surgical clip and after induction of CBD injury (top). At the bottom is shown the x-ray cholangiogram of the same animal after intra-GB injection of 5 ml of Renografin®-60. Black arrowhead indicates leakage of iodine contrast. GB: gallbladder, CBD: common bile duct, CD: cystic duct, HD: hepatic duct.